Oct 18th, 12:00 AM

Flexural Capacity of Continuous Span Standing Seam Panels: Gravity Load

Reynaud Serrette

Teoman Pekoz

Twelfth International Specialty Conference on Cold-Formed Steel Structures
St. Louis, Missouri, U.S.A., October 18-19, 1994

Flexural Capacity of Continuous Span Standing Seam Panels: Gravity Load

R. L. Serrette[1] and T. Pekōz[2]

SUMMARY

The standing seam panel is one of the most practical and economical roofing systems developed in recent years. Construction of the roof system requires that the panel legs be overlapped and crimped. Under gravity load, the crimped outstanding leg of the connected panels may be subject to distortional buckling. A design method was previously suggested for estimating the distortional buckling strength of the outstanding leg of a single simply supported standing seam panel. In this paper, an approximate method is present for estimating the capacity of a system of interconnected continuous span standing seam panels. Experimental results for three full-scale continuous span tests and one full-scale simple span test show that the approximate method provides a relatively accurate estimate the maximum capacity for a system subject to gravity load.

INTRODUCTION

Cold-formed steel panels are used extensively in the roofs of commercial and residential buildings. The panels are fabricated from light gage steel sheets and have thicknesses which typically range from 0.030 in. to 0.018 in. (22 to 26 gage). Based on their configuration, roof panels may be broadly classified as either lap seam or standing seam panels, as illustrated in Figure 1. The standing seam roof panel system differs from the lap seam system in the method in which the panels are supported and the potential for instability of the compression flange in the span. The standing seam panel is attached to underlying structural purlins using a clip which is concealed in the seam (between adjacent legs). The clip allows for a connection-free surface and provides a convenient mechanism to accommodate thermal expansion and contraction of the panel.

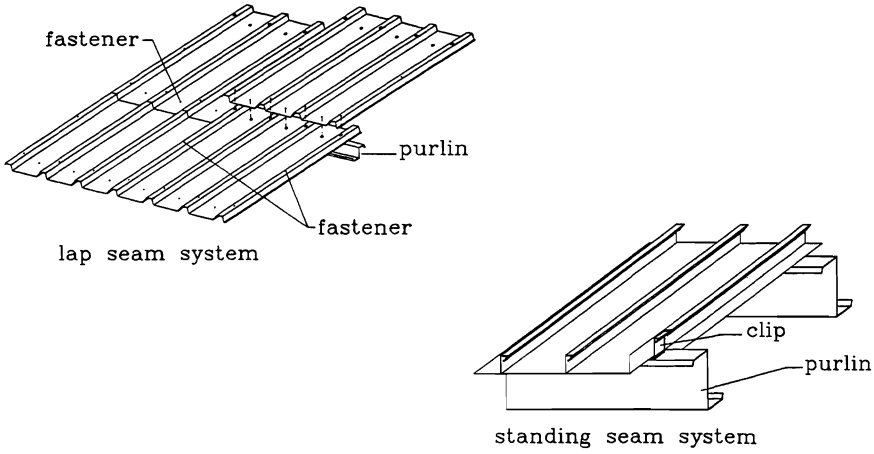

Figure 1 Roof panel systems

[1] Asst. Professor, Department of Civil Engineering, Santa Clara University, Santa Clara, CA 95053
[2] Professor, School of Civil and Environmental Engineering, Cornell University, Ithaca, NY 14853

Application-wise, the standing seam roof system has a number of advantages over the lap seam system including: (1) a continuous skin membrane, (2) an elevated seam and a water-tight system, and (3) a system that can easily withstand thermal movements without damage to insulation and the structure.

The main disadvantage of the standing seam is related to instability of the laterally unsupported compression flange(s) in the span. Serrette and Pekõz (1992) presented methods for estimating the strength of single panels with laterally unsupported compression flanges and one of the methods is used in this paper to estimate the capacity of the standing seam roof system.

DESIGN PROCEDURE

The following design procedure involves two steps to estimate the distortional buckling design stress, $\sigma_{cr,d}$, in the standing seam system. In the first step, the elastic distortional buckling stress, $\sigma_{crel,d}$, of the outstanding leg is computed using an expression presented by Serrette and Pekõz (1992). In step two, the elastic distortional buckling stress is modified to take into account inelastic behavior, using the following expressions:

$$\sigma_{cr,d} = \sigma_{crel,d} : \quad if\ \sigma_{crel,d} \le \frac{\sigma_y}{2} \tag{1}$$

$$\sigma_{cr,d} = \sigma_y \left(1 - \frac{\sigma_y}{4\sigma_{crel,d}}\right) : \quad if\ \sigma_{crel,d} > \frac{\sigma_y}{2} \tag{2}$$

The effective section modulus $\bar{S}_{eff}$ (of one unit in the system) is then calculated at the stress $\sigma_{cr,d}$ using the AISI specification (AISI, 1991). The moment capacity, M_n, for the interaction mode (local-distortional buckling) is then computed as:

$$M_n = \sigma_{cr,d}\, \bar{S}_{eff} \tag{3}$$

The following section briefly discusses the computation of the elastic distortional buckling stress, $\sigma_{crel,d}$.

ELASTIC DISTORTIONAL BUCKLING STRESS

The elastic distortional buckling stress, $\sigma_{crel,d}$, may be computed from the elastic moment capacity, $M_{crel,d}$, of the restrained outstanding leg. $M_{crel,d}$ may be estimated from the expression:

$$M_{crel,d} = \frac{\alpha_1 + \alpha_2}{\alpha_3} \tag{4}$$

where

$$\alpha_1 = (EI_{xy}\eta\theta^2)^2 \tag{5}$$

$$\alpha_2 = -(EI_x\theta^2)(EC_w\theta^2 + EI_y\eta^2\theta^2 + GJ\theta + k_\phi) \tag{6}$$

$$\alpha_3 = -(2\eta + \beta_x)(EI_x\theta^2)\theta \tag{7}$$

$$\eta = y_o - h_y \tag{8}$$

$$\theta = \frac{\pi^2}{L_e^2} \tag{9}$$

I_x, I_y, and I_{xy} define the moment of inertia about the strong (x) axis, the moment of inertia about the weak (y) axis, and the product of inertia, respectively, of the outstanding leg. β_x, J, and C_w are geometric parameters of the outstanding leg (see Serrette and Pekõz, 1992). k_ϕ defines a linear elastic rotational spring constant. (x_o, y_o) and (h_x, h_y) define the coordinates of the shear center, s, and the enforced center of rotation, n, respectively, relative to the centroid of the outstanding leg, as illustrated in Figure 2.

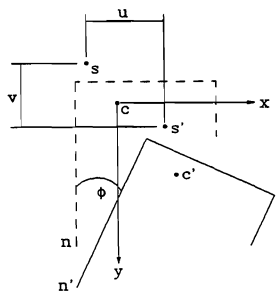

s: shear center
c: centroid
n: point on the axis of rotation

Figure 2 Outstanding leg

For a given length for the unsupported compression flange, equations (4), (5), (6), (7), (8), and (9) may be used to estimate the elastic distortional buckling stress. The effective length, L_e, of the unsupported compression flange may be taken as

$$L_e = kL_u \tag{10}$$

where k is an effective length factor and L_u is the clear unsupported length of the compression flange. For the specimens tested in this project, lateral deflection of the flange at the support was inhibited by the clips which connect the panels to the underlying purlins. Using the column effective length factors (SSRC, 1990), k of 0.65 was assumed to be adequate for the given lateral support conditions. The elastic rotational stiffness, k_ϕ, at the web-tension flange junction can be taken as:

$$k_\phi = \frac{D}{\left(\frac{w_f}{6} + \frac{w_w}{3}\right)} \qquad \text{when } w_f/t < 400 \tag{11}$$

and

$$k_\phi = \frac{D}{\left(\frac{w_f}{16} + \frac{w_w}{3}\right)} \qquad \text{when } w_f/t > \text{ or } = 400 \tag{12}$$

where

$$D = \frac{Et^3}{12\,(1-\nu^2)} \tag{12}$$

w_f = width of the tension flange
w_w = depth of the web
t = thickness of the section

The expressions given by equations (11) and (12) force a discontinuity at the w_f/t limit of 400. If there is local buckling in the web, there will be a tendency for a reduction in the rotational spring stiffness defined above. To account for this reduction, an approximate multiplicative empirical reduction factor, γ (≤ 1.0), equal to the ratio of the elastic web local buckling stress to the stress required for the web to be fully effective, should be applied to k_ϕ.

Most of the geometric properties presented in the previous equations are routinely used in design and can be readily computed. The warping constant and lateral buckling parameters, C_w and β_x respectively, require more involved calculations, but can be evaluated (see Serrette and Peköz, 1992). Because the crimped legs of the panels are not "completely" connected, computation of the geometric cross-sectional properties is somewhat difficult. However, instead of using the actual leg geometries, the crimped legs may be approximated as illustrated in Figure 3. Figure 3 shows two possible models, A and B, which were used to approximate the geometry of the connected legs in the full-scale test specimens. In model A, since the approximate legs are assumed to have the same geometry and dimensions, it may be expected that the legs will have identical elastic distortional buckling stresses. The elastic distortional buckling stress for the connected legs may then be estimated on the basis of the equivalent single leg geometry and dimensions. In model B, however, it is assumed that because the lips of the individual legs are crimped (seamed), the two legs will act as a unit. Thus, in model B, the elastic distortional buckling stress is computed for the equivalent leg geometry and dimensions, but double the actual panel thickness. Using either of the model legs shown in Figure 3, the distortional buckling stress, $\sigma_{cr,d}$, may be estimated. In the calculation of the effective section modulus, it may also be assumed that due to crimping of the lips, the flanges and lips of the male and female legs act together to resist local buckling. Thus, for the computation of the effective width of the flanges and lips, the element thickness may be taken as twice the actual panel thickness. The moment capacity, M_n, of the crimped full-scale panel member may then be estimated as described earlier.

TEST PROGRAM

The dimensions and configurations of the specimens used in this test program are representative of the sections used in industry. Two different panel profiles were tested. The geometry and nominal dimensions of the sections are given in Figure 4. The nominal material properties and overall specimen member configuration for the panels are given Table 1.

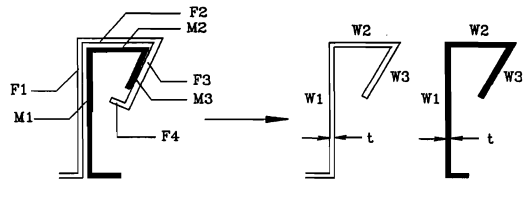

MODEL A

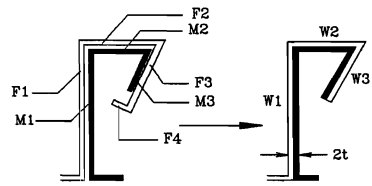

MODEL B

$W1 = \frac{F1+M1}{2}$	$W2 = \frac{F2+M2}{2}$	$W3 = \frac{F3+F4+M3}{2}$

Figure 3 Approximate models (A and B) for the crimped legs

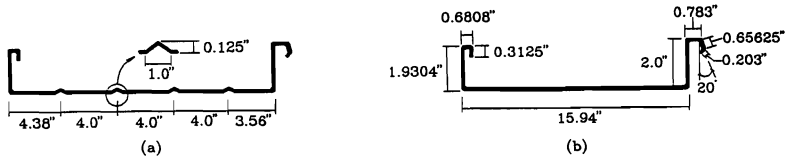

Figure 4 Configuration and dimensions of the test panels

Table 1 Overall member dimensions and material properties

Specimen Designation	Panel Cross-section	Unsupported Length of Outstanding Leg, in.	Material Yield Strength, ksi	No. of spans
SSP1-1-5.8	Figure 5 (a)	69	58	1
SSP2-3-5.0	Figure 5 (b)	60	58	3 (continuous)
SSP3-3-5.0	Figure 5 (b)	60	58	3 (continuous)
SSP4-3-5.0	Figure 5 (b)	60	58	3 (continuous)

As indicated in the above table, the full-scale test on the 16-in. standing seam panel consisted of a three (equal) span continuous beam member whereas the full-scale 20-in. panel system was tested as a single span. The basic cross-section of the full-scale roof panel specimen is illustrated in Figure 5. Each specimen was four panels wide and the panels were connected using an electric crimper.

Uniform loading of the panel assembly was achieved with a vacuum chamber built specifically for these tests. The overall layout of the vacuum chamber setup is illustrated in Figure 6. As mentioned earlier, the panels were attached to the underlying purlins using clips (typical field connection). To simulate the presence of insulation between the wide flange of the panel and the purlin, a strip of particleboard, approximately the same width as the purlin flange, was inserted in the space between the flange and the purlin.

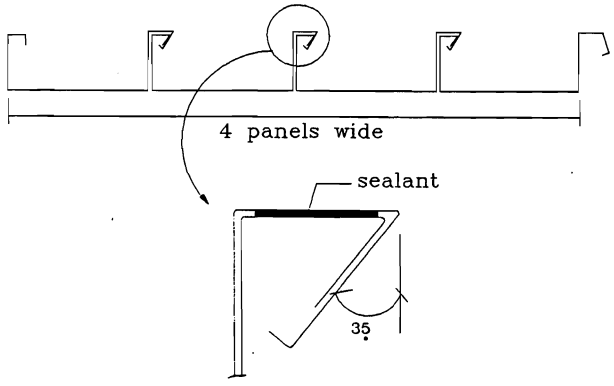

Figure 5 Cross-section of full-scale roof panel system

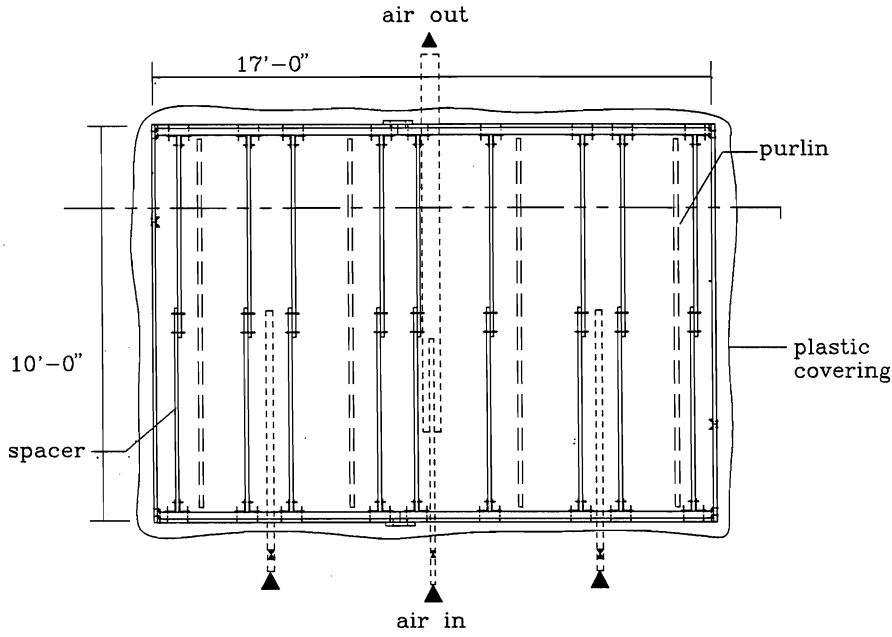

Figure 6 Overall test setup for the full-scale panel tests

Loads were applied, monotonically, to the panel member in predetermined increments until the capacity of the member was reached. Following each increment of load, the measurement devices were read and the data were stored in the computer.

The basic mode of failure for all the specimens was similar, as shown in Figure 7. For specimen SSP1-1-5.8 failure resulted from excessive lateral deflection of the compression flange mid-width in the specimen. No local buckling was observed in this specimen during the test. At the supports there was no lateral deflection of the outstanding flanges. Failure of the three span continuous specimens resulted from lateral displacement of three inner compression flanges in one of the exterior spans. Similar to the single span test, no lateral deflection of the outstanding flanges was observed at the exterior or interior supports. Prior to reaching the maximum load, flange local buckling and web crippling were observed at the interior supports. No local buckling was observed in the spans. The measured maximum capacities, w_t, of the full-scale specimens are given in Table 2.

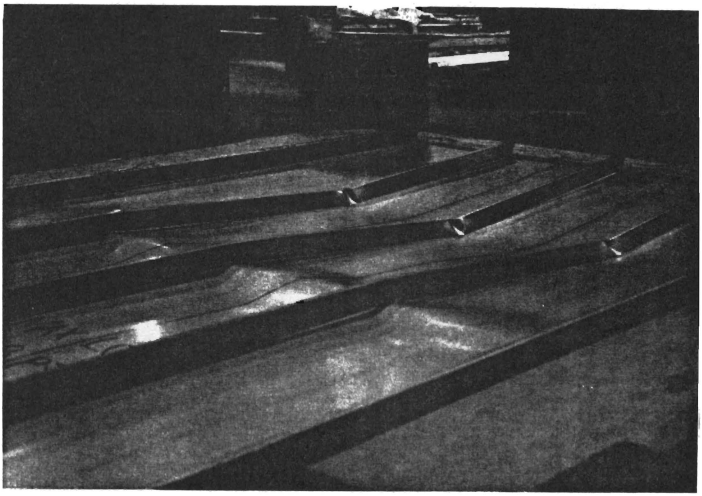

Figure 7 Mode of failure in the continuous span full-scale test

Table 2 Measured maximum capacity of the full-scale specimens

Specimen Designation	Measured Maximum Load (w_t), psf	Mode of Failure
SSP1-1-5.8	95.25	distortional buckling of middle connected leg
SSP2-3-5.0	168.83	distortional buckling in end span; flange local buckling and web crippling at the interior support
SSP3-3-5.0	168.01	"
SSP4-3-5.0	168.01	"

COMPARISON OF PREDICTED MAXIMUM CAPACITIES WITH MEASURED TEST VALUES

Using the outstanding leg models (A and B) shown in Figure 3, the distortional buckling stress may be computed as described earlier. Taking this stress as the maximum stress in the female compression flange of the crimped panel, the effective section modulus, $\bar{S}_{eff}$, for the single crimped panel may be computed.

To estimate the design moment capacity in the span, the effect of the clips supporting the panel must be taken into account. Figure 8 shows three possible models to account for the effect of the clip stiffness at the supports.

Using outstanding leg model B and the three models shown in Figure 8, the maximum uniform load capacity of the full-scale specimens were estimated and compared to the test values, and the results are presented in Table 3. The ratios in the table indicate that all the clip support models give reasonably accurate estimates of the maximum load capacity for the continuous span tests. On the other hand, the results for the one span test specimen are vastly different. For models 2 and 3 (identical models for the one span specimen), the measured maximum load capacity was 41 percent more than the predicted value while the measure capacity was only 5 percent unconservative based on model 1.

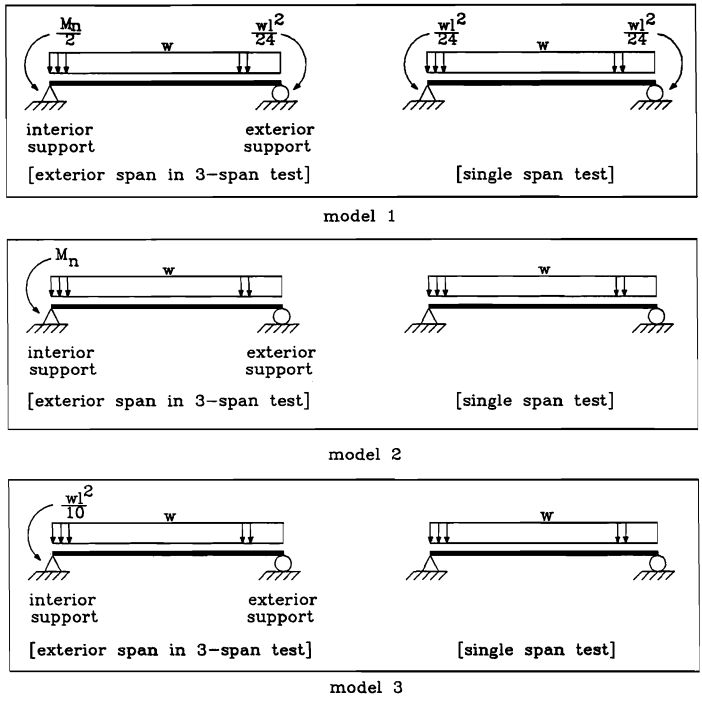

Figure 8 Models for the supports in the full-scale tests

Table 3 Comparison of the measured to predicted maximum load for the full-scale tests

Specimen Designation	Measured Maximum Load, psf	Measured Capacity / Predicted Capacity Model 1	Measured Capacity / Predicted Capacity Model 2	Measured Capacity / Predicted Capacity Model 3
SSP1-1-5.8	95.25	0.95	1.41	1.41
SSP2-3-5.0	168.83	1.00	1.05	.93
SSP3-3-5.0	168.01	0.99	1.05	.92
SSP4-3-5.0*	168.01	0.99	1.05	.92

* no clips used at the support

CONCLUSION

The design method presented for distortional buckling of standing seam roof panels systems, using outstanding leg model B for the crimped legs and the model 1 approximation flexural stiffness at the supports, gives accurate predictions of the capacity of the roof system. Some additional work may be warranted to evaluate the outstanding leg model and the clip support flexural stiffness approximations presented.

ACKNOWLEDGEMENTS

The work reported here was sponsored by the American Iron and Steel Institute. The support of AISI Task Group and its Chairman, Mr. J. Nunnery, is sincerely appreciated and gratefully acknowledged.

REFERENCES

AISI, American Iron and Steel Institute, (1991). Cold-Formed Steel Design Manual, Washington, DC, August

Serrette, R., (1992). "Behavior of Cold-Formed Steel Panels with Laterally Unsupported Compression Flanges," Dissertation, Graduate School, Cornell University, Ithaca, New York, January

Serrette, R., and Pekõz, T., (1992). "Distortional Buckling Behavior of Thin-Walled Beams." Annual Technical Session--Earthquake Stability Problems in Eastern North America, Structural Stability Research Council, Pittsburgh, Pennsylvania, April

SSRC, Structural Stability Research Council, (1990). Guide to Stability Design Criteria for Metal Structures, 4th edition, ed. T. V. Galambos. John Wiley and Sons, NY

APPENDIX I

Metric conversions:

1 psf = 47.88 Pa
1 in. = 25.40 mm
1 lb-in = 0.1130 N-m